European Journal of Neuroscience, Vol. 49, pp. 672–686, 2019 doi:10.1111/ejn.14202

Medial thalamus in the territory of oculomotor basal ganglia represents stable object value

Masaharu Yasuda[1,2] and Okihide Hikosaka[1]
[1]Laboratory of Sensorimotor Research, National Eye Institute, National Institutes of Health, Bethesda, MD, USA
[2]Department of Physiology, Kansai Medical University, 2-5-1 Shin-machi, Hirakata City, Osaka, 573-0101, Japan

Keywords: cognition, memory, monkey, reward, saccade

Abstract

Many visual objects are attached with values which were created by our long rewarding history. Such stable object values attract gaze. We previously found that the output pathway of basal ganglia from caudal-dorsal-lateral portion of substantia nigra pars reticulata (cdlSNr) to superior colliculus (SC) carries robust stable value signal to execute the automatic choice of valuable objects. An important question here is whether stable value signal in basal ganglia can influence on other inner processing such as perception, attention, emotion, or arousal than motor execution. The key brain circuit is another output path of basal ganglia: the pathway from SNr to temporal and frontal lobes through thalamus. To examine the existence of stable value signal in this pathway, we explored thalamus in a wide range. We found that many neurons in the medial thalamus represented stable value. Histological examination showed that the recorded sites of those neurons included ventral anterior nucleus, pars magnocellularis (VAmc) which is the main target of nigrothalamic projection. Consistent with the SNr GABArgic projection, the latency of value signal in the medial thalamus was later than cdlSNr, and the sign of value coding in the medial thalamus was opposite to cdlSNr. As is the case with cdlSNr neurons, the medial thalamus neurons showed no sensitivity to frequently updated value (flexible value). These results suggest that the pathway from cdlSNr to the medial thalamus influences on various aspects of cognitive processing by propagating stable value signal to the wide cortical area.

Introduction

We often find a good object after our gaze is attracted to it. Constant rewarding history creates stable values of objects which then attract our gaze (Della Libera & Chelazzi, 2009; Anderson *et al.*, 2011; Yasuda *et al.*, 2012). In this case, the gaze orientation (saccade) is automatic (Della Libera & Chelazzi, 2009; Hickey *et al.*, 2010; Anderson *et al.*, 2011) and quick (Ghazizadeh *et al*., 2016). This occurs even when objects are chosen among many (high-capacity) (Yasuda *et al.*, 2012) and even when the object had not been seen for a long time (long-term memory) (Vaughan & Greene, 1984; Strong *et al.*, 2011; Yasuda *et al.*, 2012). Such an automatic saccade is often followed by conscious object recognition.

On the other hand, our gaze can be attracted by objects by their predicted values. The behavior based on such flexible object values is based on recent experiences (short-term memory) on a small number of objects (low capacity) (Shiffrin & Schneider, 1977; Duncan, 1980). Such a conscious saccade is quickly learned and quickly forgotten (Mishkin & Delacour, 1975; Yasuda *et al.*, 2012).

Correspondence: M. Yasuda, Department of Physiology, as above. E-mail: yasudama@hirakata.kmu.ac.jp

Received 1 December 2017, revised 11 September 2018, accepted 4 October 2018

Edited by Yoland Smith. Reviewed by Anonymous and Atsushi Nambu.

All peer review communications can be found with the online version of the article.

Previously, we reported that the two forms of object values are separately processed in different circuits within the basal ganglia (Kim & Hikosaka, 2013; Yasuda & Hikosaka, 2015). The stable object value is preferentially represented in the caudal part of the basal ganglia, which is composed of the tail of caudate (CDt) and the caudal-dorsal-lateral portion of SNr (cdlSNr) (Yamamoto *et al.*, 2013; Yasuda & Hikosaka, 2015). On the other hand, the flexible object value is preferentially represented in the rostral part of the basal ganglia, which is composed of the head of caudate (CDh) and the rostral-ventral-medial portion of SNr (rvmSNr) (Kim & Hikosaka, 2013; Yasuda & Hikosaka, 2015). The parallel processing by these basal ganglia circuits would be beneficial, because it can cause a saccade quickly toward whichever object that possesses either stable or flexible value. However, in the actual environment, the stable and flexible values are sometimes different in each object, which may disrupt the saccade toward the object. To deal with this situation, the brain should have the ability to link stable value with flexible value processing.

Anatomical studies suggest that the stable value pathway has access to the flexible value pathway. It has been reported that the caudal part of SNr, which is equivalent to cdlSNr, has disynaptic projections to the prefrontal cortical areas which preferentially innervate CDh (Lynch *et al.*, 1994; Middleton & Strick, 2002; Tanibuchi *et al.*, 2009). Those signals are relayed by medial thalamic nuclei which heavily interact with a wide part of the frontal cortex (Kunzle & Akert, 1977; Ilinsky *et al.*, 1985) and receive strong inputs from

caudal SNr (Ilinsky *et al.*, 1985; Erickson *et al.*, 2004). These data suggest that the thalamus is a key structure for the interaction between stable and flexible object values.

To investigate this hypothesis, we examined neuronal representation of stable and flexible object values in a wide area of thalamus. We found that many stable-value-coding neurons were localized in the medial thalamus. Consistent with the hypothesis, the value differentiation in the medial thalamus occurred later than cdlSNr, and stable-value-coding neurons in the medial thalamus were insensitive to flexible object values, as shown in cdlSNr (Yasuda *et al.*, 2012). The recording sites of these stable-value-coding neurons included VAmc, which is a major thalamic target structure of caudal SNr (Ilinsky *et al.*, 1985). These results suggest that the medial thalamus is a critical node for coordinating behavior in complex environments which contain multiple types of object values.

Materials and methods

Subjects

Two rhesus monkeys (*Macaca mulatta*), D (male, 13 y/o, 9 kg), G (male, 15 y/o, 11 kg), were used as subjects in this study. All

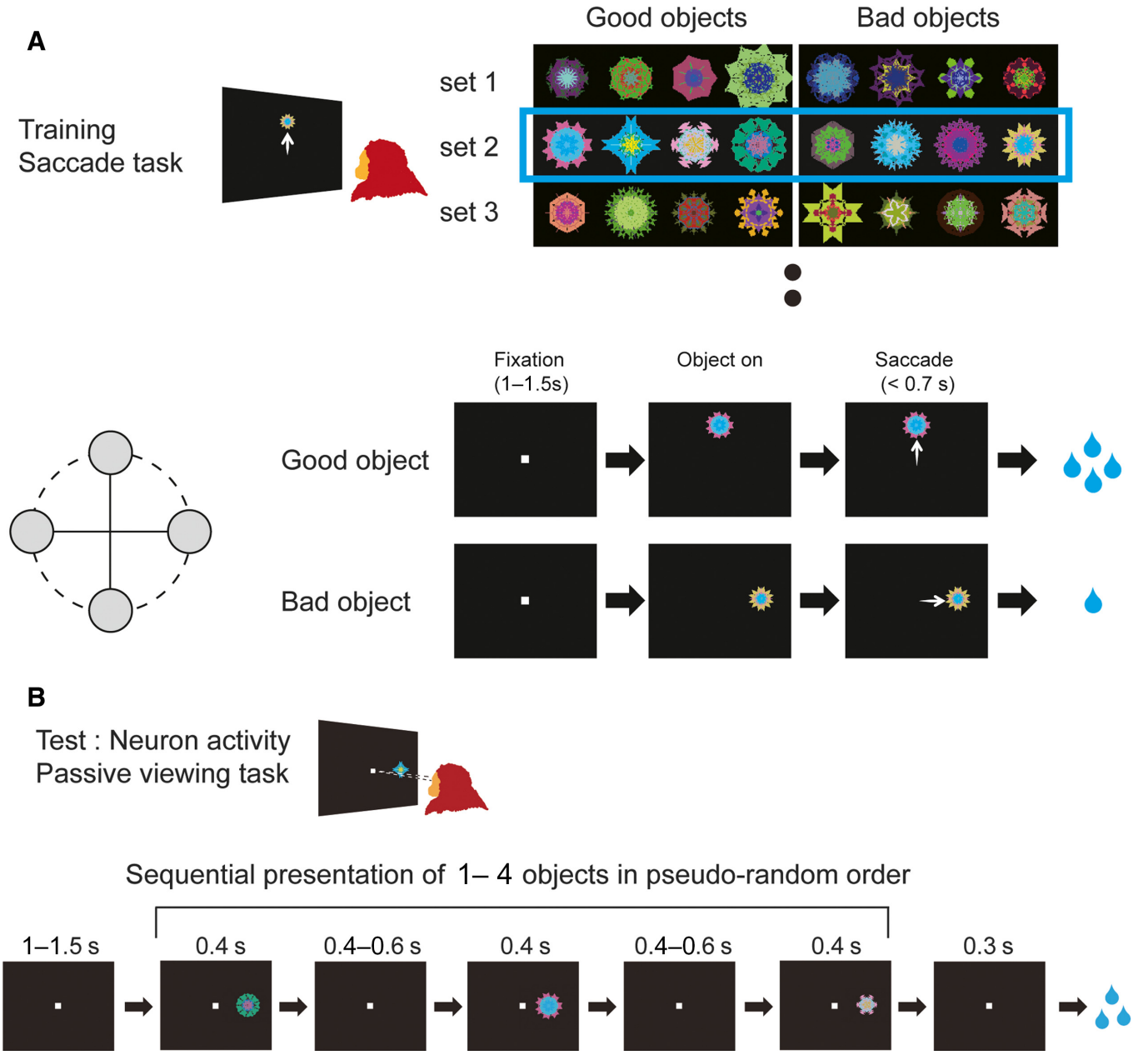

FIG. 1. Stable value procedures. (A) Behavioral learning of stable values. Visual objects were grouped into sets of eight objects. Among each set, four were assigned as 'good' objects and the other four were assigned as 'bad' objects. On each trial, one of the eight objects was presented at one of four positions, and the monkey made a saccade to it. If the object was good, a large reward was delivered. If the object was bad, a small reward was delivered. For each set of visual objects, the learning procedure was done repeatedly across many daily sessions, throughout which each object remained either good or bad. (B) Testing of neuronal activity. While the monkey was fixating a central spot of light, 1–4 fractal objects (pseudo-randomly chosen from a set of eight objects) were presented sequentially at the neuron's preferred position. The monkey was rewarded 300 ms after the final object disappeared. The reward was thus not associated with particular objects.

animal care and experimental procedures were approved by the National Eye Institute and Institutional Animal Care and Use Committee and complied with the Public Health Service Policy on the humane care and use of laboratory animals.

Surgical procedure

A plastic head holder, scleral search coils, and plastic recording chambers were implanted under general anesthesia and sterile stereotaxic surgical conditions. The monkeys were deprived of food a half day before anesthesia. Anesthesia was induced with ketamine and diazepam, after which the monkey was intubated and then maintained with isoflurane. We aimed at thalamus from both lateral and posterior chambers. Based on a stereotaxic atlas (Saleem & Logothetis, 2007), we placed two rectangular chambers in lateral and posterior location on each monkey's skull. The lateral chamber was placed over the fronto-parietal cortex (monkey G: 10 mm anterior, tilted laterally by 35°, chamber size (AP × LM), 30 × 22 mm in inner diameter; monkey D: 20 mm anterior and tilted laterally by 38°, chamber size (AP × LM), 36 × 26 mm in inner diameter). The posterior chamber was placed over the midline of the parietal cortex, tilted posteriorly (monkey G: tilted posteriorly by 38°, chamber size (AP × LM), 30 × 22 mm in inner diameter; monkey D: tilted posteriorly by 42°, chamber size (AP × LM), 21 × 19 mm in inner diameter). After the monkeys fully recovered from surgery, MR images (4.7T, Bruker) were obtained along the direction of the recording chamber which was visualized with gadolinium that filled grid holes and inside the chamber.

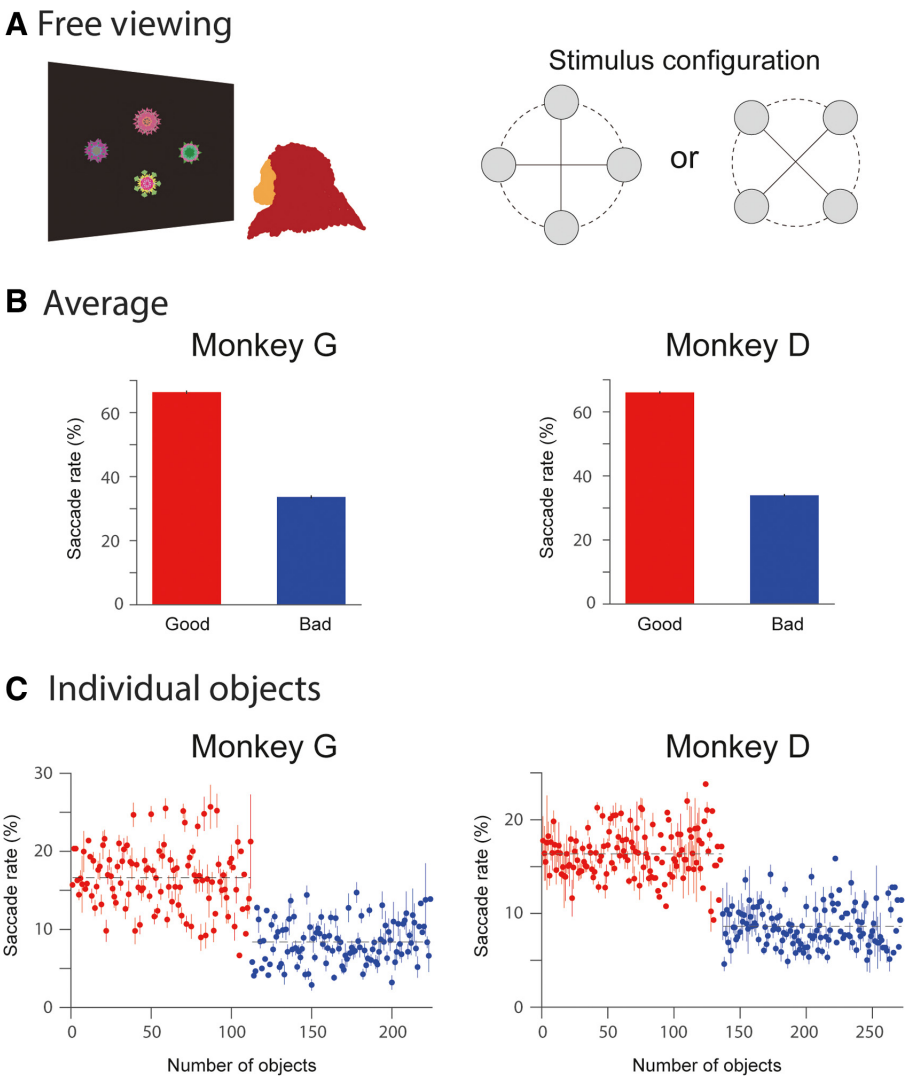

FIG. 2. High-capacity long-term memory of stable value. (A) Behavioral testing of stable value. Under free-viewing condition, four of a set of eight fractal objects were chosen pseudo-randomly and were presented in one of two configurations. Each object was presented at least 25 times in one session. A white dot, instead of fractal objects, sometimes appeared at a random position and a reward was delivered when the monkey fixated the dot. Therefore, the reward was not associated with particular fractal objects. (B) The monkeys' gaze preference to learned objects. The average of saccade rate for well-learned (≥ 5 daily training sessions) good (red bar) and bad (blue bar) objects in individual test sessions were plotted. For both monkeys, the gaze was significantly attracted by good objects (monkey G: $P \approx 0$, monkey D: $P \approx 0$, *t*-test). The gaze preference was tested at least 1 day after the final training of the tested objects to exclude the effect of short-term memory. (C) The monkeys' gaze preference across objects. The monkeys' behavior significantly discriminated many objects. Monkey G: 224 objects, *t*-test: $P = 2.0 \times 10^{-32}$, rank-sum test, mean saccade rates are 16.6 and 8.6% for good (red) and bad (blue) objects, respectively. Monkey D: 272 objects, *t*-test: $P = 1.9 \times 10^{-51}$, mean saccade rates are 16.4 and 8.4% for good (red) and bad objects (blue), respectively.

Behavioral task

Behavioral tasks were controlled by a QNX-based real-time experimentation data acquisition system (REX, Laboratory of Sensorimotor Research, National Eye Institute, National Institutes of Health (LSR/NEI/NIH), Bethesda, MD, USA). The monkey sat in a primate chair, facing a frontoparallel screen 33 cm from the monkey's eyes in a sound attenuated and electrically shielded room. Stimuli generated by an active matrix liquid crystal display projector (PJ550, ViewSonic, Walnut, CA, USA) were rear-projected on the screen. We created visual stimuli using fractal geometry (Yamamoto *et al.*, 2012). One fractal was composed of four point-symmetrical polygons which were overlaid around a common center such that smaller polygons were positioned more front. Its size was approximately 8° × 8°.

Stable object-value association procedure

The goal of this procedure was to create and test stable (long-term) memories of object-value association. To achieve this goal, each object was associated with a fixed reward value during learning. The testing procedure was performed separately with no reward contingency to exclude possible influences of flexible (short-term) memories (see Yasuda *et al.*, 2012 for details).

In learning procedure, we used an object-directed saccade task (Fig. 1A) to create a fixed bias among fractal objects in their reward values (i.e., good objects and bad objects). In each session, a set of eight fractal objects was used as the target. On each trial, one of the fractal objects was chosen pseudo-randomly as the target and was presented at one of four possible locations (right, up, left, and bottom). The monkey was required to make a saccade to the target to obtain a liquid reward. Importantly, half of the fractal objects were associated with a large reward (0.11 mL) (i.e., good objects), whereas the other half were associated with a small reward (0.02 mL) (i.e., bad objects). One training session consisted of 64 trials (eight trials for each object). For each set of objects, the reward bias was maintained throughout the present study. On each training day, monkey D and G learned 1–18 and 1–11 sets of objects, respectively. For each object set, no more than one training session was conducted in 1 day.

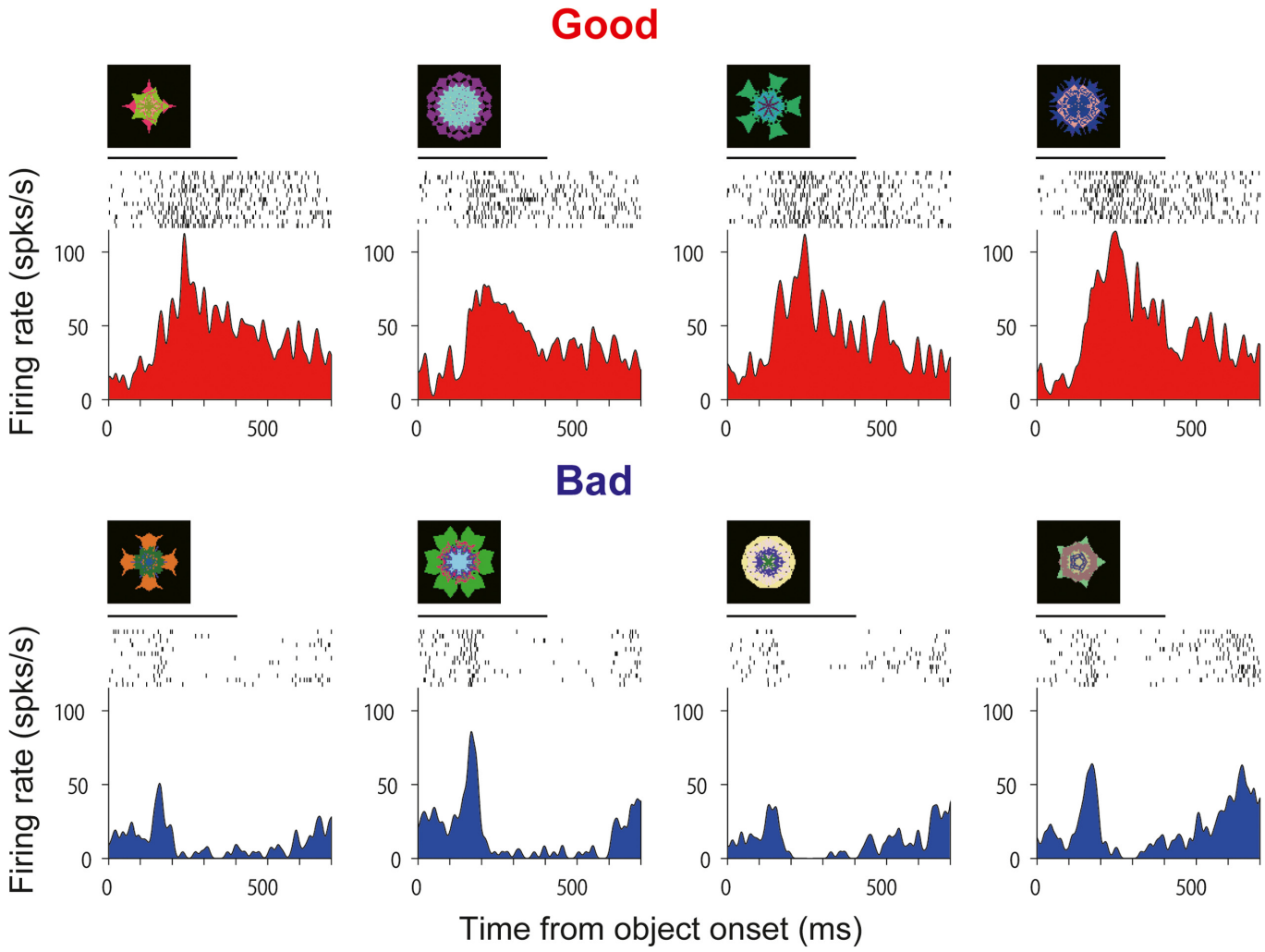

FIG. 3. Stable-value-coding of a thalamus neuron. The responses of the thalamus neuron to good objects (top) and bad objects (bottom) recorded from monkey G. For each object, spike activity of the neuron is shown by rasters of dots (top) and spike density function (bottom), which are aligned on the onset of the object (time 0). The horizontal bar shown above each raster plot indicates the duration of object presentation (0–400 ms). The objects were presented at the neuron's preferred location while the monkey was fixating at the central fixation point. The monkey had been trained with the set of objects for 41 sessions across days, and the thalamus neuron was recorded 5 days after the final day of the training session. One training session was done in 1 day.

To test the neuronal representation of stable object-value memories, we used a passive viewing task (Fig. 1B). While the monkey was fixating a central spot of light, 1–4 fractal objects (pseudo-randomly chosen from a set of eight objects) were presented in the neuron's preferred location in sequence (presentation time: 400 ms, inter-object time interval: 400–600 ms). The monkey was rewarded 300 ms after the final object disappeared. Thus, no particular objects were associated with the reward. Each object was presented at least six times in one session.

To test the behavioral representation of stable object-value memories, we used a free-viewing task (Fig. 2A; Yasuda *et al.*, 2012). On each trial, four of a set of eight fractal objects were chosen pseudo-randomly and were presented simultaneously for 2 s. The monkey was free to look at these objects (or something else) by making

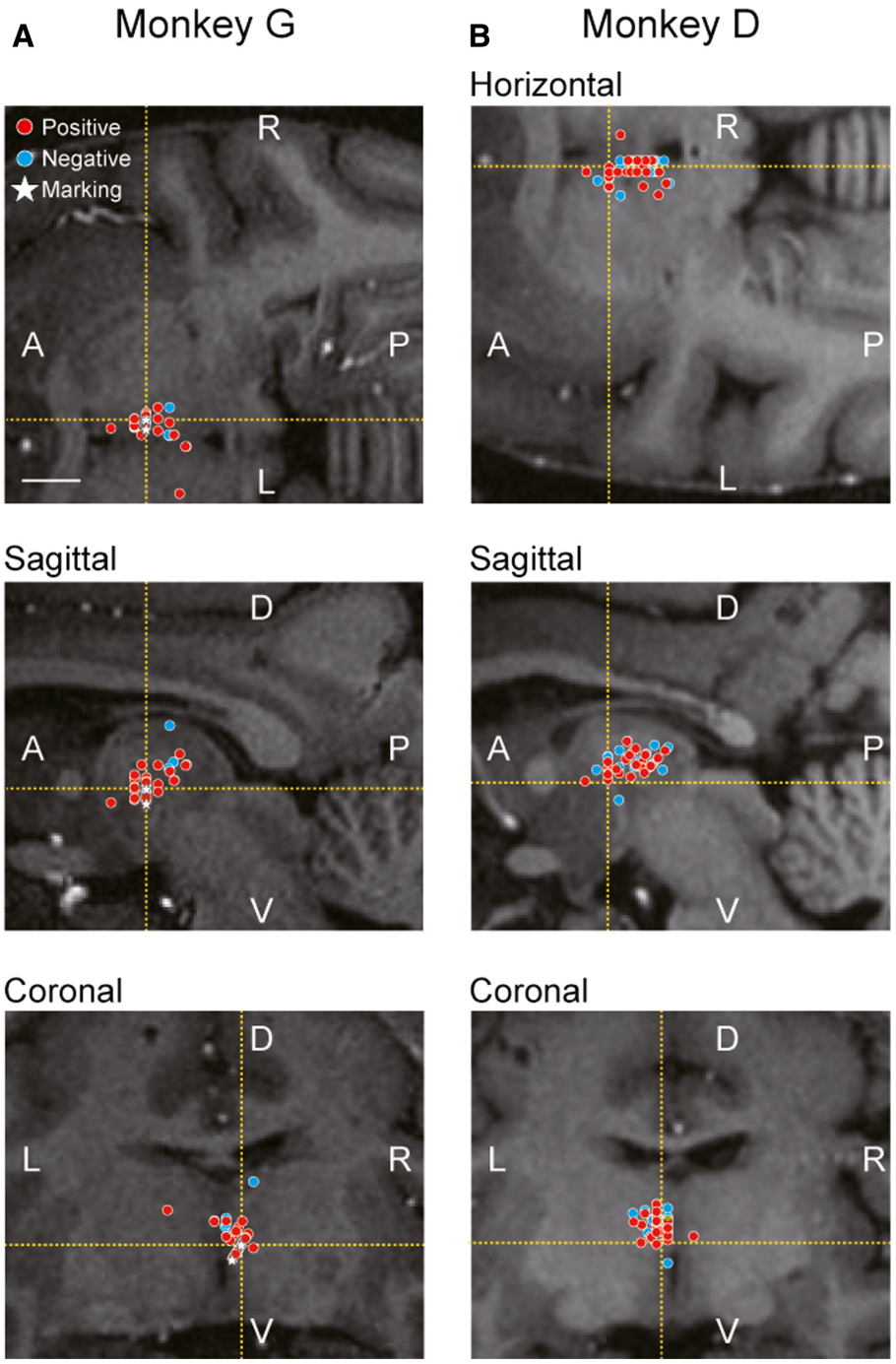

FIG. 4. The distribution of stable-value-coding neurons in the stereotaxic coordinates. Recorded sites of the neurons with positive-value-coding (red dot) and negative-value-coding (blue circle), and the locations of two marking lesions (white stars) are plotted on horizontal (0.5 mm ventral to AC for monkey G and D), sagittal (1.5 mm lateral to midline for monkey G and D), and coronal (6.25 and 5.75 mm posterior to AC for monkey G and D, respectively) sections. In monkey G (A), the dotted lines are all aligned with the dorsal one of the two marking lesions. In monkey D (B), the dotted lines are equivalent to those in monkey G, although the recording sides were mostly opposite. The white horizontal bar in the top left panel indicates 5 mm.

saccades between them, but no reward was given. After a blank period (0.5 s), another four objects were presented. Occasionally, a white small dot, instead, was presented at one of four positions. If the monkey made a saccade to it and held the gaze on it for 300–600 ms, a reward was delivered. This dot rewarded trial was used to maintain the monkey's arousal and motivation level. Each object was presented at least 25 times in one session. We also used a modified version, which was the same as the original task except that, before each fractal presentation, the white dot appeared at the center and the monkey was required to fixate it for 1000–1500 ms. To test the monkeys' long-term memory, the task was performed at least 1 day after the final training of the tested objects.

Flexible object-value association procedure

The goal of this procedure was to create and test flexible (short-term) memories of object-value association. An essential feature of short-term memory is that it can be updated frequently. Therefore, learning and testing were performed simultaneously in one task procedure (object-directed saccade task, Fig. 10A).

For each monkey, a fixed set of two fractal objects (say, A and B) was used as the saccade target. Each trial started with the appearance of a central white spot, which the monkey had to fixate on. After 1000–1500 ms while the monkey was fixating on the central spot, one of the two fractal objects was chosen pseudo-randomly and was presented at the neuron's preferred location. The fixation point (FP) disappeared 400 ms later, and then the monkey was required to make a saccade to the object within 700 ms. If the gaze was held on the object for 400 ms, a liquid reward was delivered. The monkey received a large reward (0.20 mL) after making a saccade to one object (e.g., A) and received a small reward (0.016 mL) to the other object (e.g., B). During a block of 30 trials, the object-reward contingency was fixed (e.g., A-large/B-small), but it was reversed in a following block (e.g., B-large/A-small) without any external cue. While a thalamus neuron was being recorded, these two blocks (A-large/B-small and B-large/A-small) were repeated alternatively at least twice (their order counterbalanced across neurons). Most trials (24 out of 30 trials) were forced trials: one of the two objects was presented and the monkey had to make a saccade to it. The rest of trials (6 out of 30 trials) were choice trials: two objects were presented at the same time. Their locations were chosen randomly from four possible locations (right, up, left, and bottom). The monkey had to choose one of the objects by making a saccade to it to obtain the reward associated with the chosen object. If the monkey failed to make a saccade correctly on either forced or choice trials, the same trial was repeated.

Electrophysiology

Single-unit recordings were performed using tungsten electrodes (Frederick Haer, Bowdoin, ME, USA) that were advanced by an oil-

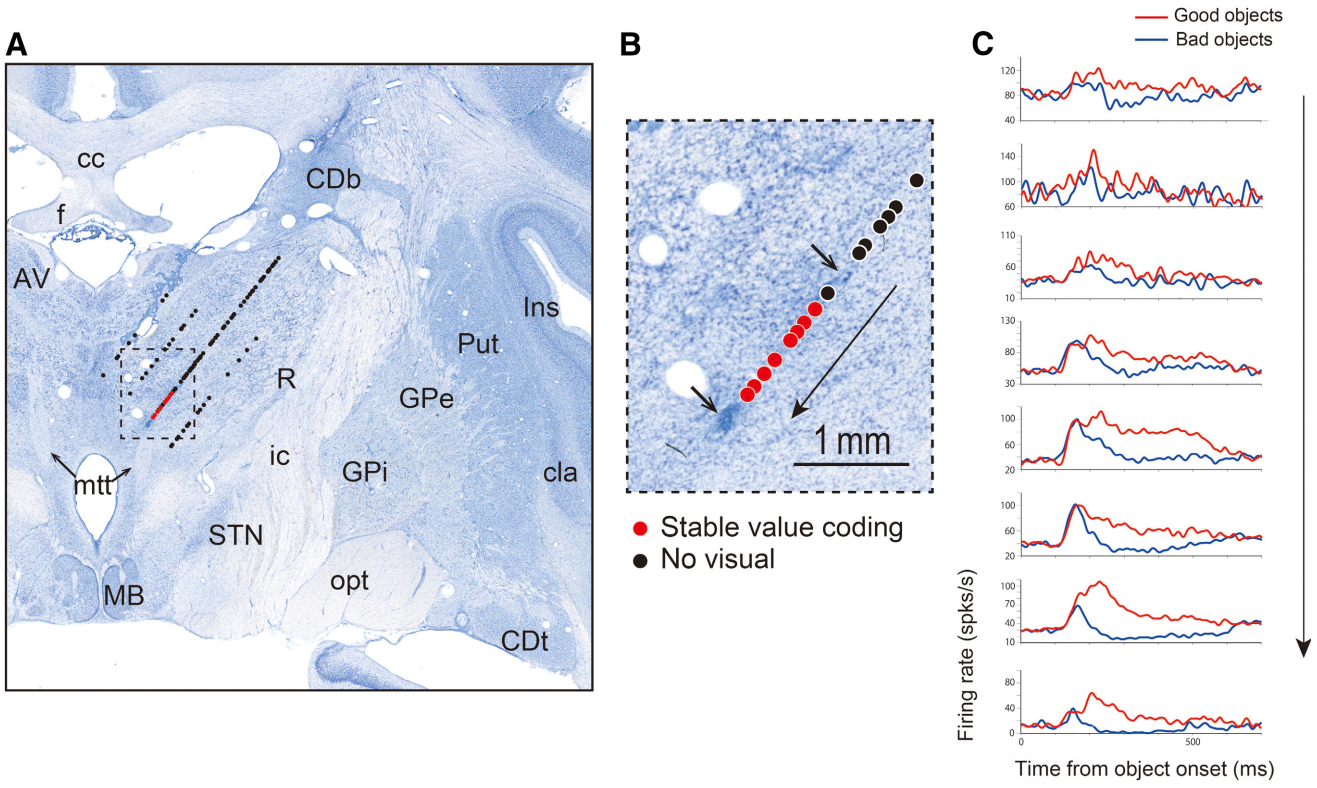

FIG. 5. Clustering of stable-value-coding neurons in VAmc thalamus. (A and B), A coronal histological section (at the level of 5.8 mm caudal to the anterior commissure, AC) overlaid with the locations of recorded neurons in four electrode penetrations for monkey G. Red dots: neurons showing visual responses with significant stable values; Black dots: neurons showing no visual response. Along the penetration, two marking lesions (arrows in B) were made at the top and bottom of the multiple stable-value-coding neurons. The mammillothalamic tract (mtt) is present near the bottom of the marking lesion. (C) The responses of stable-value-coding neurons (red dots in B) to good objects (red) and bad objects (blue). Note that the discriminability for good and bad objects was greater near the end of the penetration. The neuron in Fig. 3 is shown at the second from the bottom. (AV: anterior ventral nucleus, cc: corpus callosum, CDb: body of caudate nucleus, CDt: tail of caudate nucleus, cla: claustrum, f: fornix, GPe: globus pallidus, external segment, GPi: globus pallidus, internal segment, ic: internal capsule, Ins: insula, MB: mammillary body, mtt: mammillothalamic tract, opt: optic tract, Put: putamen, R: reticular thalamic nucleus, STN: subthalamic nucleus)

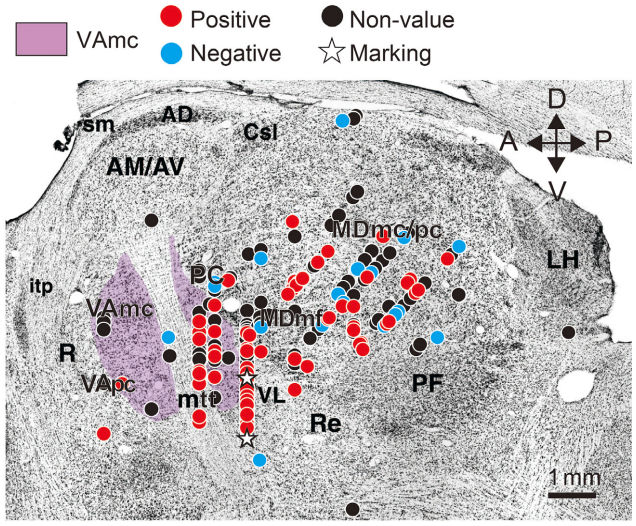

FIG. 6. The distribution of stable-value-coding neurons in thalamus. Neurons with positive-value-coding (red dot), negative-value-coding (blue dot), and non-value-coding (black dot) in two monkeys are plotted on a sagittal section (1.55 mm lateral to midline) (Ilinsky *et al.*, 2002). They are roughly separated into the anterior and posterior groups by the paracentral nucleus (PC). Note that stable-value-coding neurons are gathered around VAmc (purple area) and that the location of the lower one of two marking lesions (white star) is just above mtt, which is equivalent to the histological examination (Fig. 5). (A: anterior, D: dorsal, P: posterior, V: ventral, AD: anterodorsal nucleus, AM/AV: anteromedial/anteroventral nucleus, Csl: centralis superior nucleus lateralis, itp: internal capsule, LH: lateral habenular nucleus, MDmc: medial dorsal nucleus, pars magnocellularis, MDmf: medial dorsal nucleus, pars multiformis, MDpc: medial dorsal nucleus, pars parvicellularis, mtt: mammillothalamic tract, PC: Paracentral nucleus, PF: parafascicular nucleus, R: reticular thalamic nucleus, Re: nucleus reuniens, sm: stria medullaris, VAmc: ventral anterior nucleus, pars magnocellularis, VApc: ventral anterior nucleus, pars parvicellularis, VL: ventral lateral nucleus)

driven micro-manipulator (MO-97A; Narishige, Setagaya-ku, Tokyo, Japan). The recording sites were determined by using a grid system, which allowed recordings at every 1 mm between penetrations. In each daily experiment, we introduced these electrodes into the brain, each through a stainless steel guide tube, which was inserted into one of the grid holes and then to the brain via the dura. For finer mapping of neurons, we also used a complementary grid, which allowed electrode penetrations between the holes of the original grid. The electrical signal from the electrode was amplified with a band-pass filter (200 Hz–5 kHz; BAK, Mount Airy, MD, USA) and collected as digital signal at 1 kHz. Action potentials of single neurons were isolated online using a custom voltage–time window discrimination software (MEX, LSR/NEI/NIH).

Data analysis

We analyzed the effects of object-value association learning on neuronal and behavioral discriminations of good and bad objects. To assess the neuronal discrimination, we first measured the magnitude of thalamus neuron's response to each fractal object by counting the numbers of spikes within a test window. For both stable and flexible object value testing, we put the test window from 100 to 400 ms after the onset of the object. For each neuron, we compared response magnitudes in individual trials between good objects and bad objects to calculate the area under the receiver operating characteristic (ROC) for defining the neuronal discrimination, and to perform Wilcoxon rank-sum test for testing the statistical significance of the neuronal discrimination of learned objects. If the neuronal activity for good objects or bad objects in the test window was significantly different from the neuronal activity during a 300 ms period before the onset of the object (*t*-test, $P < 0.05$), we defined the neuron as 'visually responsive'. Otherwise, we defined the neuron as 'non-visually responsive'.

To examine possible contributions of thalamus neuronal activity to object-value learning, we first focused on the periods in which the monkey showed clear saccade biases (well-learned periods): ≥ 5 daily training sessions in stable object-value learning; ≥ 5th trials after the reversal of the object-reward contingency in flexible object-value learning.

The latency of visual response was calculated by using a bootstrap analysis. We set a sliding test window (duration: 20 ms) starting from 50 ms after object presentation. Each time we slided the test window by 1 ms, we compared the mean firing rate in the test window with time window in 100 ms period before object presentation. Trials were randomly resampled with replacements to form a new bootstrap dataset which is composed of half number of trials. Such random resampling and comparison were repeated 300 times. If the averaged discharge rate in the test window was smaller or larger than in bad object trials in 292 trials, the time point was regarded as the time of a significant separation. The beginning of six consecutive significant separations was defined as the latency of visual response.

To obtain the latency of neuronal differentiation for stable value, we made a cumulative histogram for each group of objects (i.e., good objects and bad objects). We then sought the time when the two histograms started to diverge. For this purpose, we first searched the time where the difference in the two histograms was maximum during a fixed time period after the onset of visual stimulus (50–400 ms). We set 50 ms as the starting time because any time before this is likely to be the initial visual signal unaffected by its value. We set 400 ms as the ending time when the object disappeared. We then sought backward in time where the two histograms first crossed, which we defined as the neuronal differentiation time for stable value. When we could not detect any cross point, we stopped analyzing the data for the neuron.

To assess the behavioral discrimination for learned objects, we calculated the choice rate for good objects, which was defined as follows: nSACg/(nSACg + nSACb), where nSACg and nSACb are the number of saccades toward good and bad objects, respectively. The choice rate for bad objects was defined as follows: nSACb/(nSACg + nSACb). For stable value learning, the choice rate was calculated in free-viewing task between four good and four bad objects (Fig. 2B). For flexible value learning, the choice rate was calculated in choice trial of object-directed saccade task between good (currently associated with large reward) and bad (currently associated with small reward) objects (Fig. 10). To assess behavioral and neuronal discrimination more precisely, we calculated the saccade rate (Fig. 2C) and ROC (Fig. 7D) for individual objects based on the following comparison: a particular (good or bad) object vs. other four objects which belong to the same set of eight objects, but to the opposite type of value (bad or good).

We recorded thalamus neurons' activity from posterior and lateral chambers in two monkeys. To combine the penetrations from two different chambers, we first obtained three-dimensional (3D) coordinates of two chambers by using MRI. This enabled us to plot the positions of all recorded neurons in the stereotaxic coordinates (coronal, sagittal, and horizontal) (Fig. S1 and Fig. 4). In particular, the horizontal coordinate was aligned with the anterior–posterior direction of the lateral chamber that was positioned by the stereotaxic surgery (see Surgical procedure).

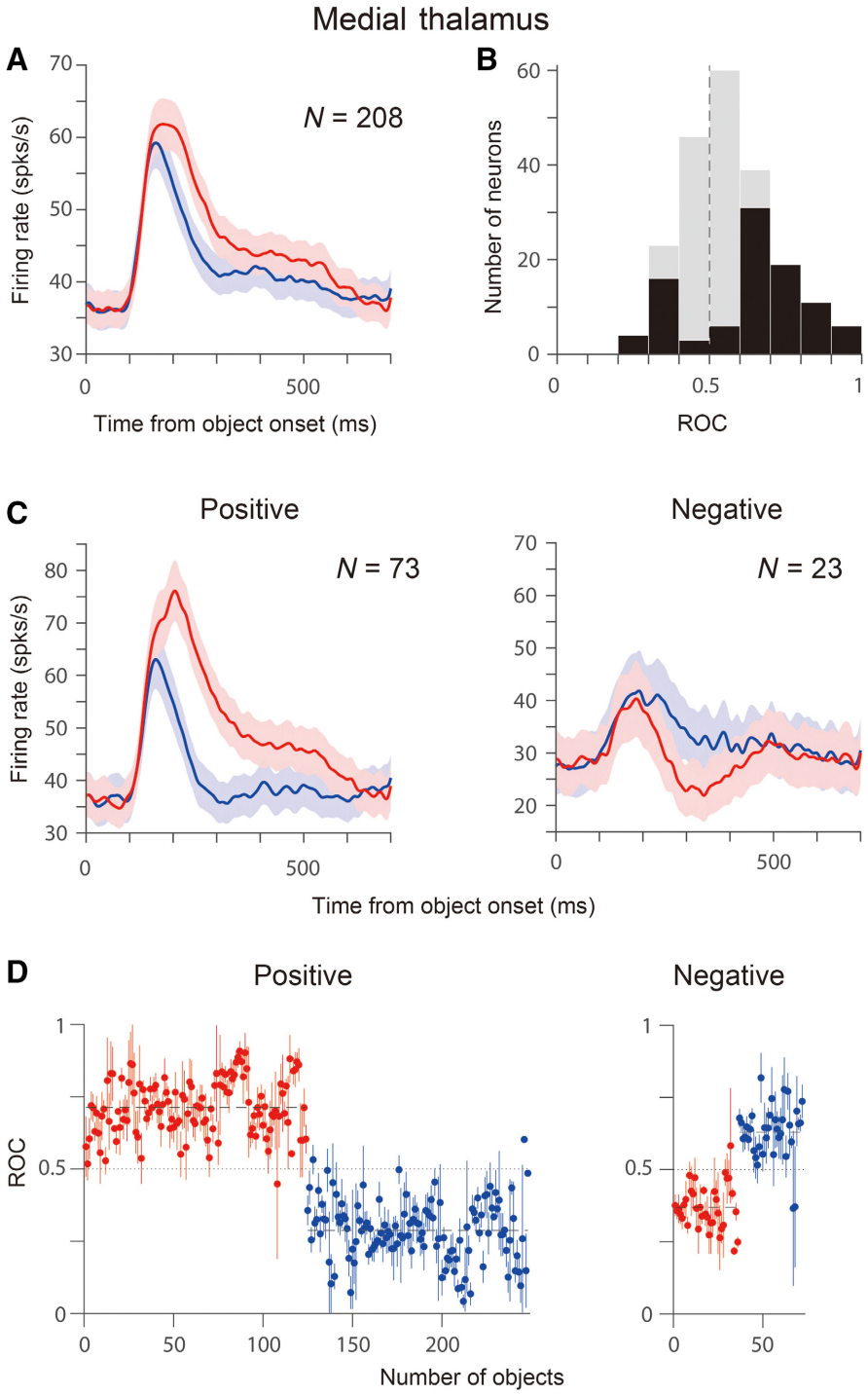

FIG. 7. Stable-value-coding of medial thalamus neurons in different groups. (A) Averaged responses of visually responsive medial thalamus neurons (n = 208) to good object (red) and bad objects (blue). The data were obtained for well-learned sets (≥ 5 training sessions). (B) Discrimination between good and bad objects in individual recording sessions measured by the area under ROC based on spike counts in a test window (100–400 ms after the onset of object). ROC>0.5: stronger response to good than bad objects (positive-value-coding); ROC<0.5: stronger response to bad than good objects (negative-value-coding). Black bars indicate neurons with statistically significant discrimination assessed by Wilcoxon rank-sum test ($P < 0.05$). (C) Averaged responses of medial thalamus neurons that showed significant discrimination of stable object value with positive-value-coding (left, n = 73) or negative-value-coding (right, n = 23). (D) Neuronal discrimination across objects. The neurons significantly discriminated individual objects based on stable value for both neuronal types (positive-value-coding: $P = 6.3 \times 10^{-42}$, rank-sum test, mean ROCs are 0.71 and 0.29 for good (red) and bad (blue) objects, respectively. Negative-value-coding: $P = 6.7 \times 10^{-12}$, rank-sum test, mean ROCs are 0.37 and 0.63 for good (red) and bad (blue) objects, respectively). The colored area in spike density function in A and C indicates standard error.

For monkey G (Fig. 4A), two marking lesions shown in Fig. 5B are indicated by white stars in each of the stereotaxic coordinates. Each of the coordinates was aligned on the plane that crossed the dorsal one of the two marking lesions (coronal, 6.25 mm posterior to anterior commissure (AC); sagittal, 1.5 mm lateral to midline; horizontal, 0.5 mm ventral to AC). Notably, the coronal MR image

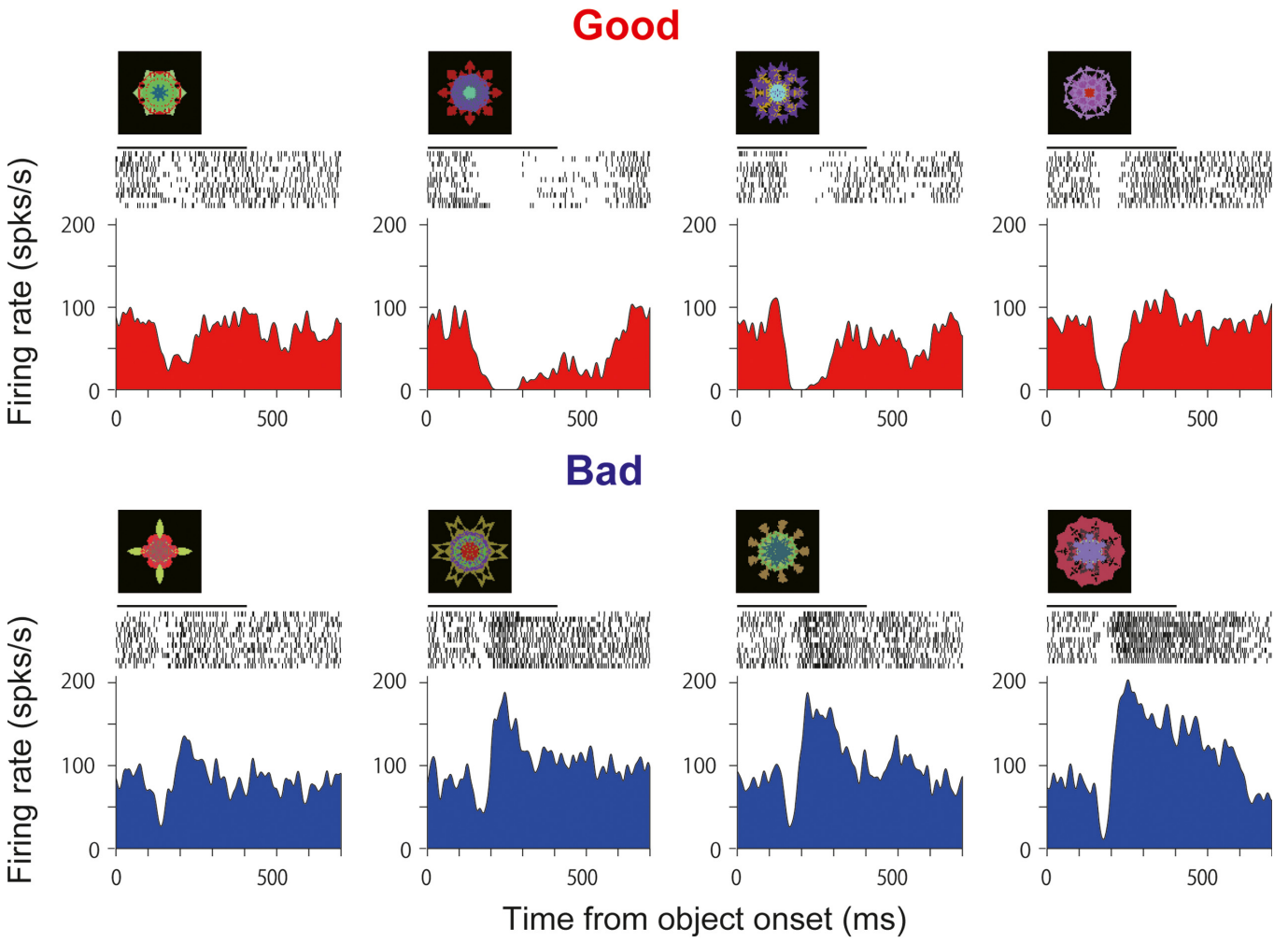

FIG. 8. Stable-value-coding of an SNr neuron. This neuron was located in the caudal-dorsal-lateral part of SNr (cdlSNr) of monkey G. The format is the same as Fig. 3. The monkey was trained with the set of objects for 13 sessions across days, and the SNr neuron was recorded 4 days after the final day of the training session. This SNr neuron and the thalamus neuron shown in Fig. 3 were recorded in the same animal.

is very similar to the histological section in Fig. 5A. For monkey D (Fig. 4B), equivalent MR images are shown in the 3D coordinates (coronal, 5.75 mm posterior to AC; sagittal, 1.5 mm lateral to midline; horizontal, 0.5 mm ventral to AC). We also overlaid neurons' coordinates onto a sagittal section image (1.55 mm from midline) of a brain atlas (Ilinsky *et al.*, 2002). To create the overlaid image, we combined neurons' coordinates for two monkeys by adjusting the coordinates of AC, and plotted them on the sagittal atlas image (1.5 mm lateral to midline) which was resized to MR section (Fig. 6).

Histology

In the later part of the experiments in monkey G, we made two electrolytic microlesions at the recording sites (13 μA; 30 s). In anterior and medial-ventral part of thalamus, we found a 'hot spot' where many stable-value-coding neurons were concentrated. We chose the beginning and end of the hot spot for the microlesions along a penetration track from lateral chamber. The animal was then deeply anesthetized with an overdose of pentobarbital sodium and perfused transcardially with saline followed by 4% paraformaldehyde. The head was fixed to the stereotaxic frame, and the brain was cut into blocks in the coronal plane including thalamic region. The block was post-fixed overnight at 4 °C, and then cryoprotected for 5 days in increasing gradients of glycerol solutions (5, 10–20% glycerol in PBS) before being frozen. Frozen block was cut every 50 μm using microtome. The sections were stained with cresyl violet (see Fig. 5).

Results

Our hypothesis is that stable value signals represented in SNr influences cognitive function. To test this, we created stable value by letting two monkeys be engaged in long-term training to learn the values of many visual objects by using a reward biased saccade task (Fig. 1A). Many visual objects were grouped into sets of eight objects. For each set, the monkey was trained for many days (monkey G: 1–59 days, monkey D: 1–39 days). In each set, four objects were associated with a large reward (good objects), while the other four were associated with a small reward (bad objects). The object-value contingency was fixed across the whole training schedule. New sets of objects were introduced step by step during the days of training. Overall, monkey G learned 131 sets (1048 objects) and monkey D learned 133 sets (1064 objects).

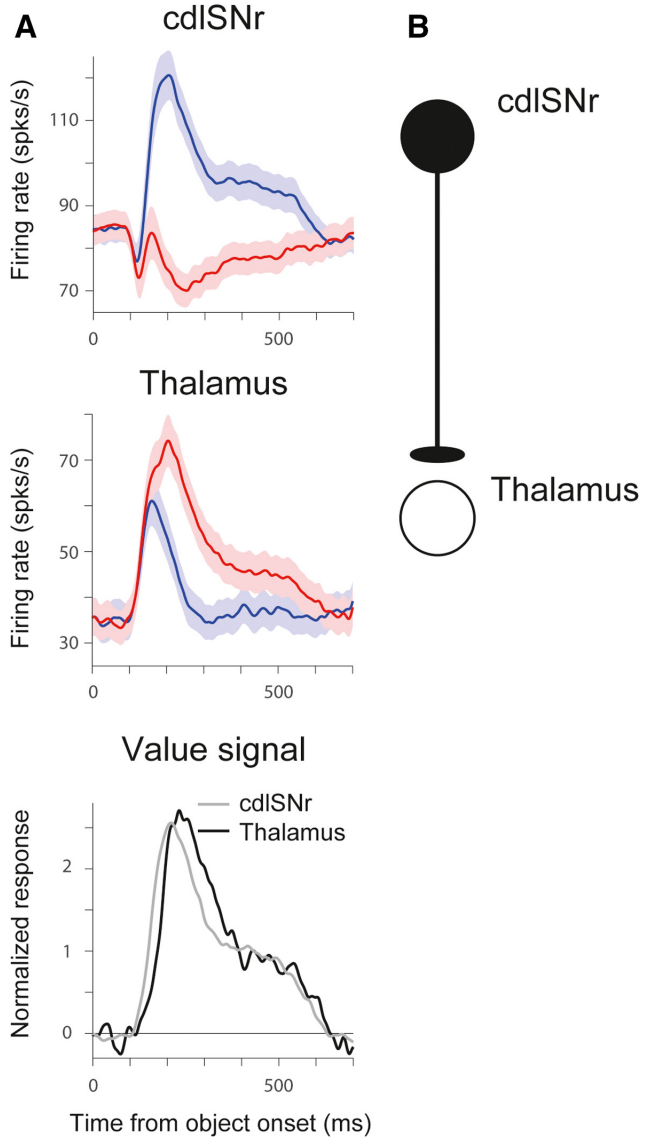

FIG. 9. Comparison of stable-value-coding between cdlSNr and medial thalamus. (A) Average responses of stable-value-coding cdlSNr neurons (top) (Yasuda *et al.*, 2012) and medial thalamus neurons (middle) to good object (red) and bad objects (blue). Bottom: Difference between the response to good objects and the response to bad objects in cdlSNr neurons (gray) and medial thalamus neurons (black). The firing rate was normalized by *Z*-score. The polarity is reversed: bad-good for cdlSNr, good-bad for thalamus. The latency of the averaged visual response is longer in medial thalamus neurons (122 ms) than cdlSNr neurons (110 ms) ($P = 0.03$, *t*-test). The latency of the averaged value differentiation is also longer in medial thalamus neurons (159 ms) than cdlSNr neurons (132 ms ($P = 5.3 \times 10^{-10}$, *t*-test). The colored area in spike density function indicates standard error. (B) Hypothesis: Stable values of visual objects are transmitted from cdlSNr to medial thalamus by inhibitory connections.

To test the monkeys' memory of stable value, we presented learned objects under free-viewing condition (Fig. 2A). During free-viewing, the monkeys' gaze was attracted by good objects. This tendency became gradually stronger across training days, and reached plateau after five training sessions (days) (well-learned; see Materials and methods). We tested 272 and 224 well-learned objects for monkey D and G, respectively. Both monkeys tended to make the saccade to good objects than bad objects (Fig. 2B, *t*-test: $P \approx 0$ for monkey D and G). We also found that the value-based saccade preference was present for individual objects (Fig. 2C, *t*-test: $P = 1.9 \times 10^{-51}$ for monkey D, $P = 2.0 \times 10^{-32}$ for monkey G), suggesting that they have acquired high-capacity memory of stable object value.

Previously, we found that cdlSNr neurons robustly encoded stable object values (Yasuda *et al.*, 2012). Anatomical studies indicate that SNr also sends signals to the frontal cortex indirectly through the thalamus (Ilinsky *et al.*, 1985; Middleton & Strick, 1994). To examine the signal processing in the SNr-thalamus pathway, we focused on the reward value coding of thalamus neurons. We first tested the visual response of the recorded neuron. For two monkeys, we plotted the recorded sites of visually responsive neurons on MR images. As shown in Fig. S1, the recording sites are well-matched to thalamic region and were widely distributed (monkey G: 4.3 mm dorsal to 5 mm ventral from AC-PC line, 3.3–12.6 mm posterior to AC, −0.6 to 4.0 mm lateral to midline; monkey D: 3.7 mm dorsal to 5.2 mm ventral from AC-PC line, 3.8–12.4 mm posterior to AC, 0–6.4 mm lateral to midline). We then examined whether the neuron encoded object values stably by using a passive viewing task (test session, Fig. 1B). The objects were presented one at a time in the neuron's receptive field (somewhere in the contralateral hemifield). To exclude any short-term reward effect, a reward was delivered randomly in no association with any particular object. Moreover, the test session was done at least 1 day after the training.

We found that a group of thalamus neurons encoded stable value. Example responses to a single set of eight objects are shown in Fig. 3. The neuron preferentially responded to the visual stimulus when it was presented in contralateral visual field (left of FP). The neuron was strongly excited by all of four good objects. In response to all of four bad objects, the neuron was initially excited, but then inhibited. The monkey had learned the object set 41 times (days) before the recording, and the neuron was tested 5 days after the final day of the learning session. The neuron also showed the similar value representation for two other sets of 16 objects. This means that the neuron retained the values of the 24 objects stably, at least for 5 days. In the whole thalamus, 96 out of 208 visually responsive neurons (43 out of 110 for monkey G, 53 out of 98 for monkey D) showed the stable-value-coding.

The stable-value-coding neurons were relatively localized in the thalamus. The overlaid plot of stable-value-coding neurons onto MR images (Fig. 4) showed that many stable-value-coding neurons were localized in medial portion of thalamus (which we call "medial thalamus" below). In two monkeys, more than 75% of them were located within 2 mm from midline (monkey G: 93%, monkey D: 76%). This was confirmed by histological examination, as exemplified in Fig. 5. Among four electrode penetrations at this anterior–posterior level (5.8 mm caudal to the AC), we found stable-value-coding neurons in only one of them. To identify their locations, we made two marking lesions at the top and bottom of the recording site where we found multiple stable-value-coding neurons, which were later revealed in a coronal histological section (Fig. 5A and B). The stable-value-coding neurons (red dots) were clustered within this restricted region (1.5 mm).

Figure 5C shows the visual responses of the stable-value-coding neurons. All of them showed stronger responses to good objects (red) than bad objects (blue), similar to the neuron shown in Fig. 3 (which is shown at the second from the bottom in Fig. 5C). Within this restricted region, the stable-value-coding was weak near the top, but became stronger near the bottom (Fig. 5C).

No neuronal activity was detected below the stable-value-coding region, which turned out to be within or around the mammillothalamic tract (Fig. 5A, mtt). This indicates that the stable-value-coding neurons were distributed near the bottom of the thalamus. According to

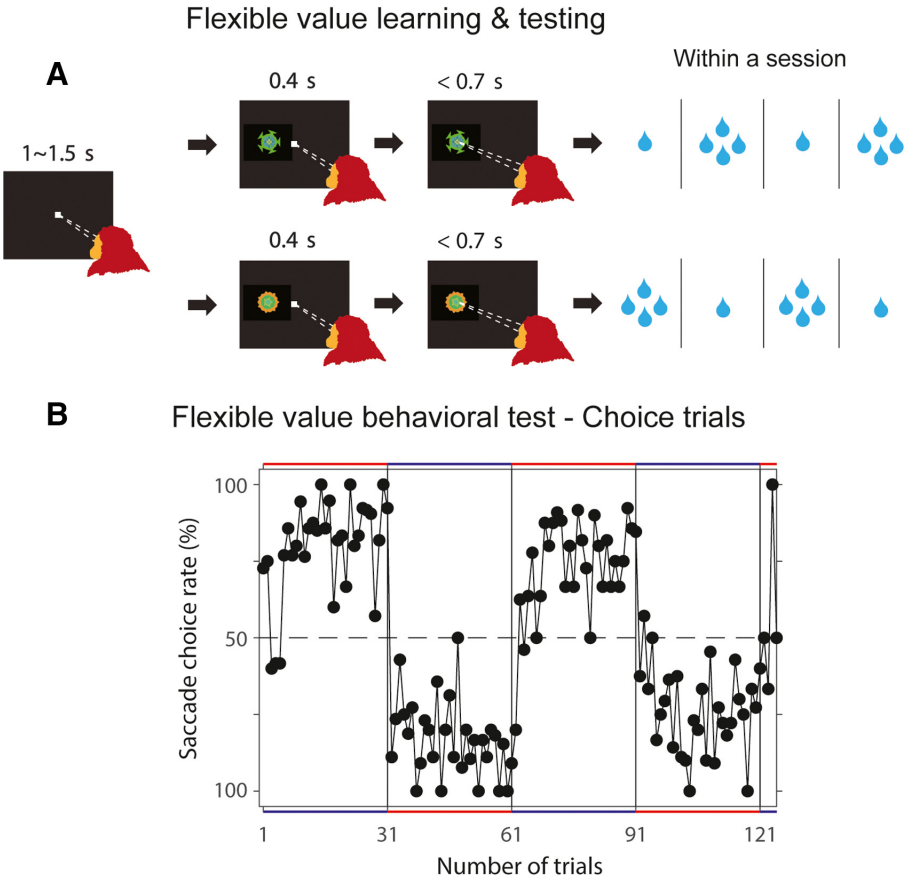

FIG. 10. Flexible value testing procedure. (A) Flexible value task. The monkey was required to hold gaze on the fixation spot until it was turned off (overlap period: 400 ms) and then make a saccade to the object. Two fractal objects were associated with large and small rewards in a reversible manner in blocks of trials (1 block: 30 trials). The objects were presented at the preferred location of the recorded neuron. Occasionally (one of five trials) two objects were presented and the monkey had to choose one of them (choice trials, not shown). (B) Flexible change of the monkeys' choice. The averaged choice rate for two monkeys is plotted against each trial. The plots close to the horizontal red bars indicate choices preferring the good object (recently associated with large reward).

the histological section, the stable-value-coding neurons were located in the ventral anterior nucleus, pars magnocellularis (VAmc). As VAmc is known to be a main target of wide area of SNr (Carpenter *et al.*, 1976; Ilinsky *et al.*, 1985; Francois *et al.*, 2002; Tanibuchi *et al.*, 2009), the stable value signal may be transmitted from cdlSNr to VAmc. In Fig. 6, the locations of stable-value-coding neurons were overlaid on a sagittal section (1.55 mm from midline) of a brain atlas (Ilinsky *et al.*, 2002). The distribution included VAmc, and also overlapped with MD, which is another major recipient of SNr input (Ilinsky *et al.*, 1985; Deniau & Chevalier, 1992; Francois *et al.*, 2002).

As a population, visually responsive neurons in the medial thalamus (n = 208) were more strongly excited by good objects than by bad objects (Fig. 7A). To quantify their stable-value-coding, we calculated ROC for individual neurons (Fig. 7B), which shows that almost half of neurons significantly differentiated stable values (96/208) (stable-value-coding neuron: $P < 0.05$, Wilcoxon rank-sum test). In particular, the distribution of ROC was biased toward 1 ($P = 8.5 \times 10^{-10}$, t-test), indicating that positive-value-coding (ROC>0.5, $P < 0.05$, Wilcoxon rank-sum test) was more common. The average activity of the positive-value-coding neurons is shown in Fig. 7C (left panels). The neurons were excited by both good and bad objects initially, but then the responses were differentiated by a steep inhibition to the bad objects (blue) and a continued excitation to good objects (red). On the other hand, the negative-value-coding neurons (n = 23, 24%), on the average, were inhibited by good objects (Fig. 7C, right panels).

Figure 7D shows the average response of medial thalamus neurons to individual objects, separately for the positive- and negative-value-coding neurons. The data indicate that medial thalamus neurons as a whole discriminated virtually all objects by their stable values. This is consistent with the value-based saccade preference for each monkey (Fig. 2C). These data together suggest that medial thalamus neurons contribute to the high-capacity memory of stable object value which causes saccades to good objects.

As we mentioned above, some SNr neurons are known to have direct inhibitory connections to thalamus neurons (Di Chiara *et al.*, 1979; MacLeod *et al.*, 1980; Miyamoto & Jinnai, 1994; Kha *et al.*, 2001; Bodor *et al.*, 2008). If the stable-value-coding of medial thalamus neurons is caused by the inhibitory connection, SNr neurons should encode stable values, but in the opposite polarities. Indeed, this is what we found in cdlSNr neurons previously (Yasuda *et al.*, 2012). In monkey G, we recorded activity of cdlSNr neurons (e.g., Fig. 8) as well as thalamus neurons (e.g., Fig. 3). The cdlSNr neuron was clearly inhibited by all four good objects and mostly excited by all four bad objects (Fig. 8). This response pattern was present in population. Averaged response of cdlSNr neurons showed clear excitation to bad objects and inhibition to good objects (Fig. 9A top, cited from Yasuda *et al.*, 2012). These cdlSNr neurons would disinhibit (and excite) thalamus neurons in response to good objects and strongly inhibit thalamus neurons in response to bad objects (Fig. 9B), which is consistent with the average activity of thalamus neurons (Fig. 9A middle).

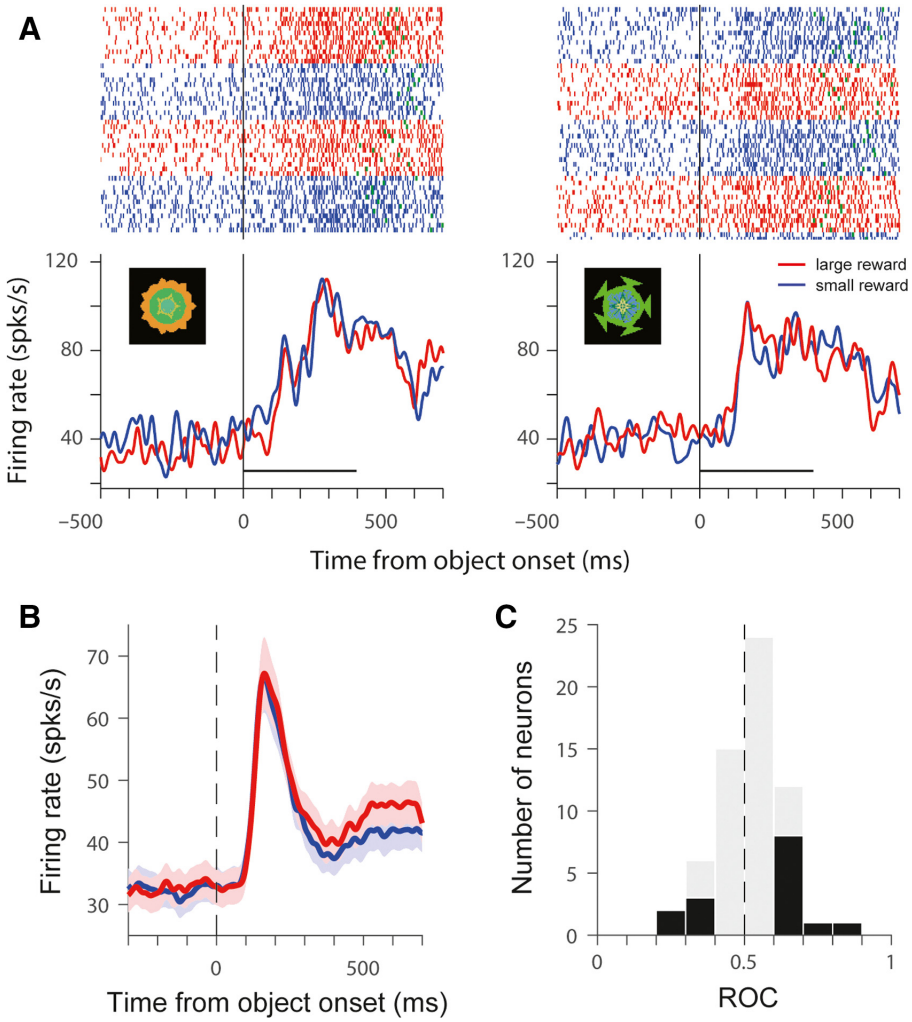

FIG. 11. Weak neuronal coding of flexible object value. (A) Spike activity of a medial thalamus neuron during the flexible value task recorded from monkey G. Its responses to the two objects are shown separately across four blocks of trials, as rasters of spikes (top) and spike density function (bottom), which are aligned on the onset of the object (time 0). The black horizontal bars indicate the overlap period (0–400 ms). Each object changed its value across blocks: good—recently associated with a large reward (red), bad—recently associated with a small reward (blue). The green dot in each raster line indicates the onset of the saccade toward the presented object. The data were obtained from the same neuron shown in Fig. 3. (B) Average activity of a population of thalamus neurons (n = 59) for two monkeys during the flexible value task, shown separately when the objects were good (red) and when the objects were bad (blue). The colored area in spike density function indicates standard error. (C) Discrimination between good and bad objects in individual neurons measured by ROC. The same format as Fig. 7B.

If the stable-value-coding in medial thalamus neurons is derived from cdlSNr, the value differentiation in cdlSNr neurons should precede that in medial thalamus neurons. To examine this possibility, we compared the time course of stable-value-coding between these two areas for individual neurons (Fig. 9A). The first phase of visual response, which showed no value bias, was an inhibition in cdlSNr neurons and an excitation in medial thalamus neurons: SNr (mean ± SD 89 ± 30 ms) vs. Medial thalamus (mean ± SD 113 ± 30 ms), $P = 4.4 \times 10^{-5}$, t-test. Then, the value differentiation started first in cdlSNr neurons and then in medial thalamus neurons: SNr (mean ± SD 130 ± 34 ms) vs. Medial thalamus (mean ± SD 170 ± 47 ms), $P = 1.8 \times 10^{-5}$, t-test. This difference is shown clearly by the value-based difference in population neuronal activity (cdlSNr: Bad - Good, medial thalamus: Good - Bad) (Fig. 9A, bottom).

So far, we have focused on the neuronal responses to stably retained object values. However, the value of a visual object could change flexibly, for example, if the amount of reward associated with the object changes. We previously found that the stable-value-coding neurons in cdlSNr did not encode flexibly changing object values (flexible value) (Yasuda *et al.*, 2012). On the other hand, some neurons in the rvmSNr encode flexible values, but not stable values, and both groups project to SC (Yasuda & Hikosaka, 2015). These results raise a question: Do the value-sensitive medial thalamus neurons receive inputs from the both groups of SNr neurons? If so, the medial thalamus neurons should encode both stable and flexible values.

To address this question, we examined the activity of medial thalamus neurons using a flexible value task (Fig. 10A). In every trial, one of two fractal objects (object A and B) was presented in the neuron's receptive field, to which the monkey made a saccade. The monkey received a large reward with object A and a small reward with object B. This set of object-reward association was reversed in every 30 trials. Thus, both objects A and B changed their values flexibly. To test monkey's preference, occasionally two objects were presented simultaneously. The monkey was required to choose one of them by making a saccade to receive reward, which was determined by chosen object. As shown in Fig. 10B, the monkeys

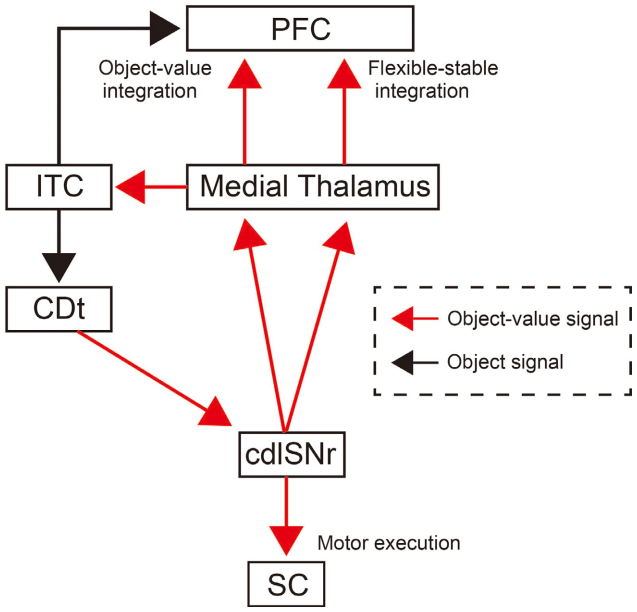

FIG. 12. Schematic diagram of the signal flow of stable object value. Stable object-value signal from cdlSNr is utilized in two different ways: (i) motor execution through the superior colliculus (SC), (ii) integrative function in the prefrontal cortex (PFC). Stable object-value signal to PFC, which is mediated by medial thalamus, may be integrated with signals for flexible behavior in PFC. This may also influence visual object signals from the inferotemporal cortex (ITC).

quickly reversed their choice preference in several trials after object-reward contingency was reversed, suggesting the monkeys flexibly changed their behavior as the objects changed their values.

Figure 11A shows the response of one medial thalamus neuron which was shown to encode stable values in Fig. 3. The neuron was excited after either one of the two objects appeared, but its response showed no change when the objects changed their values (red: good, blue: bad) (Fig. 11A). This result indicates that the neuron did not encode flexible value, even though it clearly encoded stable value (Fig. 3). This response pattern was present in population (Fig. 11B). As a population, we tested flexible-value-coding for 59 medial thalamus neurons, 57 of which were tested with both flexible and stable value. Many of them did not encode flexible value (Fig. 11C): 30 out of 43 (70%) stable-value-coding neurons, 12 out of 14 (86%) non-stable-value-coding neurons. Note that their activity became slightly differential later (> 250–300 ms) (Fig. 11B), which is also the case in stable-value-coding cdlSNr neurons (Yasuda *et al.*, 2012, fig. 14). These results suggest that SNr sends stable value signals, rather than flexible value signals, to the medial thalamus. This is probably mediated by neurons in cdlSNr, not rvmSNr. However, this does not exclude the possibility that flexible values are sent from rvmSNr to different parts of the thalamus.

Discussion

The parallel processing in basal ganglia thalamocortical loop and those functional significance has long been advocated (Alexander *et al.*, 1986). However, few recording studies were performed in line with such parallel circuits (Tanibuchi *et al.*, 2009). In the present study, we showed several lines of evidence which support signal processing of stable value from SNr to thalamus. We found stable-value-coding neurons in medial parts of the thalamus. Most of them were excited more strongly by good objects than by bad objects, which may reflect the change in the inhibitory input from cdlSNr neurons (Fig. 9). Indeed, during the recording in VAmc, we frequently observed non-isolated background activity which represented similar stable-value-coding to cdlSNr neurons (unpublished observation). Medial thalamus neurons were not sensitive to flexibly changing value. When objects changed their values frequently, medial thalamus neurons were excited by both good and bad objects (Fig. 11), which may also reflect the unchanged inhibition of cdlSNr neurons (Yasuda *et al.*, 2012; fig. 13). Anatomical studies have shown that the caudal part of SNr including cdlSNr projects to the ventral anterior nucleus of thalamus (VA), especially magnocellular division (VAmc). This thalamic area is exactly where we found stable-value-coding neurons (Fig. 5). These data suggest that stable value information is sent from cdlSNr to these thalamus neurons (Fig. 12). Our finding may be important first step to characterize the functional significance of a part of the basal ganglia thalamocortical loop.

We previously reported that rostral-ventral-medial SNr (rvmSNr) preferentially represents flexible value with little sensitivity to stable value (Yasuda & Hikosaka, 2015). Anatomical studies showed that SNr including rostral portion sends direct projection to thalamus (Carpenter *et al.*, 1976; Ilinsky *et al.*, 1985; Francois *et al.*, 2002; Middleton & Strick, 2002; Tanibuchi *et al.*, 2009). Therefore, it was unexpected that medial thalamic neurons differentiated stable value, but not flexible value. The population data in the present study showed that medial thalamic neurons encoded stable value in both positive and negative ways. Such bimodal representation was also observed in rvmSNr. Some neurons in rvmSNr represented stable value, and they were equally divided into positive-value-coding and negative-value-coding, while the most of stable-value-coding neurons in cdlSNr were negative-value-coding (Yasuda & Hikosaka, 2015; Fig. 4B). In this study, we tested flexible value coding for a confined population of neurons. There is still a possibility that stable and flexible value signals parallelly reach to different part of the thalamus. This remains an important question for future research.

Common circuit models show that the basal ganglia have two types of output: brainstem motor circuit and thalamocortical circuit (Kemel *et al.*, 1988; Hikosaka *et al.*, 2000; Deniau *et al.*, 2007). However, there has been no experiment, to our knowledge, that tested whether the same or different information is sent to the two target areas. Our previous and current studies suggest that a particular output area of the basal ganglia—cdlSNr—sends the same information to the two targets—SC and thalamus (Fig. 12).

Our data then raise an important question: Do SC and thalamus control the same or different behaviors? As the output to the brainstem motor circuit, cdlSNr sends stable value information to SC, which guides the subject to choose good objects by making saccades to them, while avoiding bad objects (Kim *et al.*, 2017). As the output to the thalamocortical circuit, cdlSNr sends the same stable value information to the thalamus. However, this may not indicate that the thalamocortical circuit controls saccades. We hypothesize possible behavioral effects of cdlSNr–thalamus circuit: memory integration and teaching. Details will be discussed below.

Memory integration

The medial thalamic areas are known to have direct connections with prefrontal cortical areas (PFC) (Ilinsky *et al.*, 1985; Middleton & Strick, 1994; Tanibuchi *et al.*, 2009). PFC plays a prominent role in 'working memory' which is a cognitive system (e.g., change behavior flexibly based on recent experiences). In contrast, medial thalamic neurons encode stable value based on long-term memory (not flexible value based on short-term memory including working memory).

It is suggested that so-called flexible behaviors often rely on stable long-term memories. For example, Wisconsin card sorting test or Stroop test are prominent behavioral procedures to test cognitive flexibility (Jensen, 1965; Chelune & Baer, 1986). To perform these tests successfully, we need to switch between two contexts flexibly, but performing in each context depends on stable long-term memory. In fact, PFC neurons switch their responses to visual stimuli between two contexts in a task similar to Wisconsin card sorting test and their responses are very stable in each context (Sakagami *et al.*, 2001). The input from cdlSNr to PFC through the medial thalamic areas may play an important role to combine short-term memory and long-term memory to make appropriate decisions in real life (Fig. 12).

There may be another place where short-term and long-term memories are combined. In addition to PFC, VAmc projects to the head of the caudate nucleus (CDh) (McFarland & Haber, 2001) which encode flexible values based on short-term memories (Kim & Hikosaka, 2013). This suggests that stable value signal interacts with the signal for short-term memory in multiple places in the brain.

Teaching by basal ganglia

Neurons in the medial thalamus and cdlSNr share several kinds of information, including object discrimination and value discrimination. The main part of the brain that discriminate visual objects is the inferotemporal cortex (ITC) which is tightly connected with PFC, especially the ventrolateral PFC (vlPFC) (Seltzer & Pandya, 1989; Saleem *et al.*, 2014). Stable value information mediated by the cdlSNr-medial thalamus–vlPFC circuit may enable vlPFC to combine two kinds of information: object discrimination and value discrimination. By repeating the combination, synaptic plasticity may occur in vlPFC neurons in the 'object discrimination' input from ITC based on the 'value discrimination' input from the medial thalamus, as previously hypothesized (Ashby *et al.*, 1998, 2010) (Fig. 12). In fact, many neurons in vlPFC learn and encode stable values (Ghazizadeh *et al.*, 2018b). These data suggest that the basal ganglia play an important role in teaching the cerebral cortex by providing value information. In the other perspective, this suggests that PFC becomes capable of controlling behavior and mind by integrating a variety of information, as the cognitive center.

ITC receives inputs from CDt by multi-synaptic connections through the caudal SNr and VAmc (Middleton & Strick, 1996) as a cortico-basal ganglia loop circuit.

Importantly, stable (not flexible) object value is encoded along the basal ganglia circuit: CDt (Kim & Hikosaka, 2013; Yamamoto *et al.*, 2013), cdlSNr (Yasuda & Hikosaka, 2015), and VAmc (current data). Then, the input from VAmc may enable ITC to combine 'value discrimination' information (Fig. 12), which is supported by our recent study using fMRI (Ghazizadeh *et al.*, 2018a). However, there has been no data showing that ITC neurons encode stable object values.

Supporting Information

Additional supporting information can be found in the online version of this article:

Fig. S1. The distribution of visually responsive neurons in the stereotaxic coordinates.

Acknowledgements

We thank H. F. Kim, A. Ghazizadeh, I. Monosov, D. McMahon, and H. Amita for discussions, and A. M. Nichols, M. K. Smith, T. W. Ruffner, D. Parker, G. Tansey, I. Bunea, J. W. McClurkin, L. P. A. V. Hays for technical assistance. This research was supported by the Intramural Research Program at the National Institutes of Health, National Eye Institute.

Conflict of interest

No conflicts of interest, financial or otherwise, are declared by the authors.

Data accessibility

Supporting data are available on request; please contact our research institute: Laboratory of Sensorimotor Research, National Eye Institute, NIH Building 49, Room 2A50 49 Convent Drive Bethesda, Maryland 20892-4435.

Author contributions

M.Y. and O.H. designed research; M.Y. performed research; M.Y. analyzed data; M.Y. and O.H. wrote the paper.

Abbreviations

A, anterior; AD, anterodorsal nucleus; AM/AV, anteromedial/anteroventral nucleus; AV, anterior ventral nucleus; cc, corpus callosum; CDb, body of caudate nucleus; CDh, head of caudate nucleus; cdlSNr, caudal-dorsal-lateral portion of substantia nigra pars reticulate; CDt, tail of caudate nucleus; cla, claustrum; Csl, centralis superior nucleus lateralis; D, dorsal; f, fornix; GPe, globus pallidus, external segment; GPi, globus pallidus, internal segment; ic, internal capsule; Ins, insula; itp, internal capsule; LH, lateral habenular nucleus; MB, mammillary body; MD, medial dorsal nucleus; MDmc, medial dorsal nucleus, pars magnocellularis; MDmf, medial dorsal nucleus, pars multiformis; MDpc, medial dorsal nucleus, pars parvicellularis; mtt, mammillothalamic tract; opt, optic tract; P, posterior; PC, Paracentral nucleus; PF, parafascicular nucleus; Put, putamen; R, reticular thalamic nucleus; Re, nucleus reuniens; rvmSNr, rostral-ventral-medial portion of substantia nigra pars reticulate; sm, stria medullaris; SNr, substantia nigra pars reticulate; STN, subthalamic nucleus; V, ventral; VAmc, ventral anterior nucleus, pars magnocellularis; VApc, ventral anterior nucleus, pars parvicellularis; VL, ventral lateral nucleus.

References

Alexander, G.E., DeLong, M.R. & Strick, P.L. (1986) Parallel organization of functionally segregated circuits linking basal ganglia and cortex. *Annu. Rev. Neurosci.*, **9**, 357–381.

Anderson, B.A., Laurent, P.A. & Yantis, S. (2011) Value-driven attentional capture. *Proc. Natl. Acad. Sci. USA*, **108**, 10367–10371.

Ashby, F.G., Alfonso-Reese, L.A., Turken, A.U. & Waldron, E.M. (1998) A neuropsychological theory of multiple systems in category learning. *Psychol. Rev.*, **105**, 442–481.

Ashby, F.G., Turner, B.O. & Horvitz, J.C. (2010) Cortical and basal ganglia contributions to habit learning and automaticity. *Trends Cogn. Sci.*, **14**, 208–215.

Bodor, A.L., Giber, K., Rovo, Z., Ulbert, I. & Acsady, L. (2008) Structural correlates of efficient GABAergic transmission in the basal ganglia-thalamus pathway. *J. Neurosci.*, **28**, 3090–3102.

Carpenter, M.B., Nakano, K. & Kim, R. (1976) Nigrothalamic projections in the monkey demonstrated by autoradiographic technics. *J. Comp. Neurol.*, **165**, 401–415.

Chelune, G.J. & Baer, R.A. (1986) Developmental norms for the Wisconsin Card Sorting test. *J. Clin. Exp. Neuropsychol.*, **8**, 219–228.

Della Libera, C. & Chelazzi, L. (2009) Learning to attend and to ignore is a matter of gains and losses. *Psychol. Sci.*, **20**, 778–784.

Deniau, J.M. & Chevalier, G. (1992) The lamellar organization of the rat substantia nigra pars reticulata: distribution of projection neurons. *Neuroscience*, **46**, 361–377.

Deniau, J.M., Mailly, P., Maurice, N. & Charpier, S. (2007) The pars reticulata of the substantia nigra: a window to basal ganglia output. *Prog. Brain Res.*, **160**, 151–172.

Di Chiara, G., Porceddu, M.L., Morelli, M., Mulas, M.L. & Gessa, G.L. (1979) Evidence for a GABAergic projection from the substantia nigra to

the ventromedial thalamus and to the superior colliculus of the rat. *Brain Res.*, **176**, 273–284.
Duncan, J. (1980) The locus of interference in the perception of simultaneous stimuli. *Psychol. Rev.*, **87**, 272–300.
Erickson, S.L., Melchitzky, D.S. & Lewis, D.A. (2004) Subcortical afferents to the lateral mediodorsal thalamus in cynomolgus monkeys. *Neuroscience*, **129**, 675–690.
Francois, C., Tande, D., Yelnik, J. & Hirsch, E.C. (2002) Distribution and morphology of nigral axons projecting to the thalamus in primates. *J. Comp. Neurol.*, **447**, 249–260.
Ghazizadeh, A., Griggs, W., & Hikosaka, O. (2016). Object-finding skill created by repeated reward experience. *J. Vis.*, **16**, 17.
Ghazizadeh, A., Griggs, W., Leopold, D.A. & Hikosaka, O. (2018a) Temporal-prefrontal cortical network for discrimination of valuable objects in long-term memory. *Proc. Natl. Acad. Sci. USA*, **115**, 2135–2144.
Ghazizadeh, A., Hong, S. & Hikosaka, O. (2018b) Prefrontal cortex represents long-term memory of object values for months. *Curr. Biol.*, **28**, 2206–2217 e2205.
Hickey, C., Chelazzi, L. & Theeuwes, J. (2010) Reward guides vision when it's your thing: trait reward-seeking in reward-mediated visual priming. *PLoS One*, **5**, e14087.
Hikosaka, O., Takikawa, Y. & Kawagoe, R. (2000) Role of the basal ganglia in the control of purposive saccadic eye movements. *Physiol. Rev.*, **80**, 953–978.
Ilinsky, I.A., Jouandet, M.L. & Goldman-Rakic, P.S. (1985) Organization of the nigrothalamocortical system in the rhesus monkey. *J. Comp. Neurol.*, **236**, 315–330.
Ilinsky, I.A., Kultas-Ilinsky, K. & Knosp, B. (2002). *Stereotactic Atlas of the Macaca Mulatta Thalamus and Adjacent Basal Ganglia Nuclei*. Springer Science, New York.
Jensen, A.R. (1965) Scoring the Stroop test. *Acta Physiol.*, **24**, 398–408.
Kemel, M.L., Desban, M., Gauchy, C., Glowinski, J. & Besson, M.J. (1988) Topographical organization of efferent projections from the cat substantia nigra pars reticulata. *Brain Res.*, **455**, 307–323.
Kha, H.T., Finkelstein, D.I., Tomas, D., Drago, J., Pow, D.V. & Horne, M.K. (2001) Projections from the substantia nigra pars reticulata to the motor thalamus of the rat: single axon reconstructions and immunohistochemical study. *J. Comp. Neurol.*, **440**, 20–30.
Kim, H.F. & Hikosaka, O. (2013) Distinct basal ganglia circuits controlling behaviors guided by flexible and stable values. *Neuron*, **79**, 1001–1010.
Kim, H.F., Amita, H. & Hikosaka, O. (2017) Indirect pathway of caudal basal ganglia for rejection of valueless visual objects. *Neuron*, **94**, 920–930 e923.
Kunzle, H. & Akert, K. (1977) Efferent connections of cortical, area 8 (frontal eye field) in *Macaca fascicularis*. A reinvestigation using the autoradiographic technique. *J. Comp. Neurol.*, **173**, 147–164.
Lynch, J.C., Hoover, J.E. & Strick, P.L. (1994) Input to the primate frontal eye field from the substantia nigra, superior colliculus, and dentate nucleus demonstrated by transneuronal transport. *Exp. Brain Res.*, **100**, 181–186.
MacLeod, N.K., James, T.A., Kilpatrick, I.C. & Starr, M.S. (1980) Evidence for a GABAergic nigrothalamic pathway in the rat. II. Electrophysiological studies. *Exp. Brain Res.*, **40**, 55–61.
McFarland, N.R. & Haber, S.N. (2001) Organization of thalamostriatal terminals from the ventral motor nuclei in the macaque. *J. Comp. Neurol.*, **429**, 321–336.
Middleton, F.A. & Strick, P.L. (1994) Anatomical evidence for cerebellar and basal ganglia involvement in higher cognitive function. *Science*, **266**, 458–461.
Middleton, F.A. & Strick, P.L. (1996) The temporal lobe is a target of output from the basal ganglia. *Proc. Natl. Acad. Sci. USA*, **93**, 8683–8687.
Middleton, F.A. & Strick, P.L. (2002) Basal-ganglia 'projections' to the prefrontal cortex of the primate. *Cereb. Cortex*, **12**, 926–935.
Mishkin, M. & Delacour, J. (1975) An analysis of short-term visual memory in the monkey. *J. Exp. Psychol. Anim. Behav. Proc.*, **1**, 326–334.
Miyamoto, Y. & Jinnai, K. (1994) The inhibitory input from the substantia nigra to the mediodorsal nucleus neurons projecting to the prefrontal cortex in the cat. *Brain Res.*, **649**, 313–318.
Sakagami, M., Tsutsui, K., Lauwereyns, J., Koizumi, M., Kobayashi, S. & Hikosaka, O. (2001) A code for behavioral inhibition on the basis of color, but not motion, in ventrolateral prefrontal cortex of macaque monkey. *J. Neurosci.*, **21**, 4801–4808.
Saleem, K.S. & Logothetis, N.K. (2007). *A Combined MRI and Histology Atlas of the Rhesus Monkey Brain in Stereotaxic Coordinates*. Academic Press, London.
Saleem, K.S., Miller, B. & Price, J.L. (2014) Subdivisions and connectional networks of the lateral prefrontal cortex in the macaque monkey. *J. Comp. Neurol.*, **522**, 1641–1690.
Seltzer, B. & Pandya, D.N. (1989) Frontal lobe connections of the superior temporal sulcus in the rhesus monkey. *J. Comp. Neurol.*, **281**, 97–113.
Shiffrin, R.M. & Schneider, W. (1977) Controlled and automatic human information processing: II. Perceptual learning, automatic attending, and a general theory. *Psychol. Rev.*, **84**, 127–190.
Strong, P.V., Christianson, J.P., Loughridge, A.B., Amat, J., Maier, S.F., Fleshner, M. & Greenwood, B.N. (2011) 5-hydroxytryptamine 2C receptors in the dorsal striatum mediate stress-induced interference with negatively reinforced instrumental escape behavior. *Neuroscience*, **197**, 132–144.
Tanibuchi, I., Kitano, H. & Jinnai, K. (2009) Substantia nigra output to prefrontal cortex via thalamus in monkeys. I. Electrophysiological identification of thalamic relay neurons. *J. Neurophysiol.*, **102**, 2933–2945.
Vaughan, W. & Greene, S.L. (1984) Pigeon visual memory capacity. *J. Exp. Psychol.*, **10**, 256–271.
Yamamoto, S., Monosov, I.E., Yasuda, M. & Hikosaka, O. (2012) What and where information in the caudate tail guides saccades to visual objects. *J. Neurosci.*, **32**, 11005–11016.
Yamamoto, S., Kim, H.F. & Hikosaka, O. (2013) Reward value-contingent changes of visual responses in the primate caudate tail associated with a visuomotor skill. *J. Neurosci.*, **33**, 11227–11238.
Yasuda, M. & Hikosaka, O. (2015) Functional territories in primate substantia nigra pars reticulata separately signaling stable and flexible values. *J. Neurophysiol.*, **113**, 1681–1696.
Yasuda, M., Yamamoto, S. & Hikosaka, O. (2012) Robust representation of stable object values in the oculomotor Basal Ganglia. *J. Neurosci.*, **32**, 16917–16932.